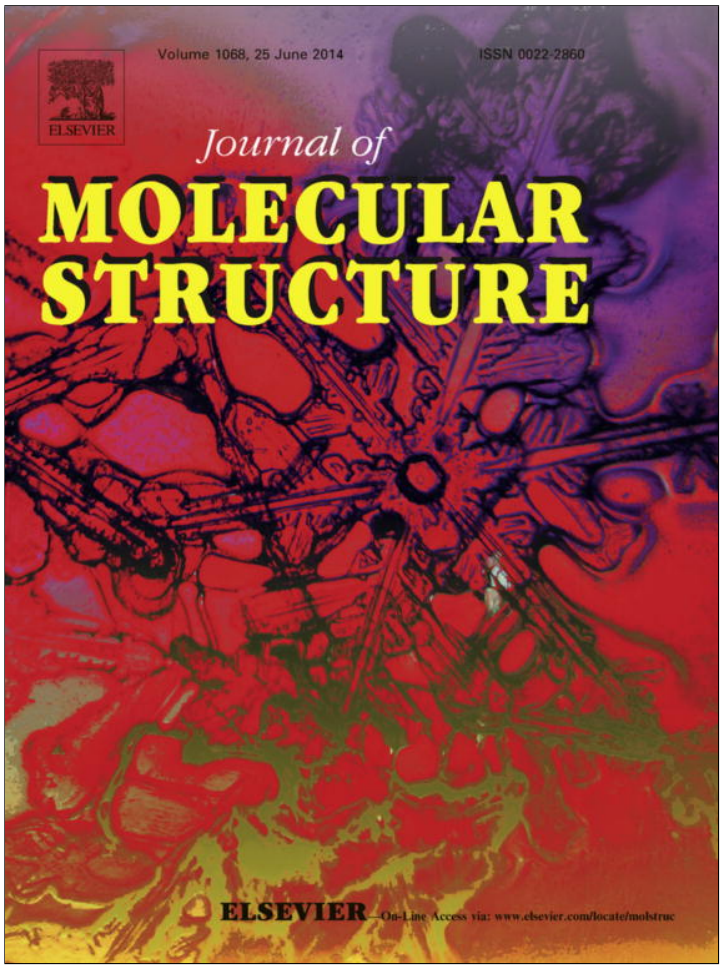

Journal of Molecular Structure 1068 (2014) 43–52

Contents lists available at ScienceDirect

Journal of Molecular Structure

journal homepage: www.elsevier.com/locate/molstruc

Aripiprazole salts IV. Anionic plus solvato networks defining molecular conformation

Eleonora Freire [a,*,1], Griselda Polla [b], Ricardo Baggio [b]

[a] Gerencia de Investigación y Aplicaciones, Centro Atómico Constituyentes, Comisión Nacional de Energía Atómica and, Escuela de Ciencia y Tecnología, Universidad Nacional General San Martín, Buenos Aires, Argentina
[b] Gerencia de Investigación y Aplicaciones, Centro Atómico Constituyentes, Comisión Nacional de Energía Atómica, Buenos Aires, Argentina

HIGHLIGHTS

- The crystal and molecular structure of five new crystalline salts of Aripiprazole are analyzed.
- The conformations found for the Aripiprazole moieties in the phosphates are different to those in previously reported salts.
- The influence on molecular conformation of the anionic/solvato network types is discussed.

ARTICLE INFO

Article history:
Received 5 February 2014
Received in revised form 20 March 2014
Accepted 21 March 2014
Available online 1 April 2014

Keywords:
Aripiprazole salts
Crystal structures
Anionic/solvate network

ABSTRACT

Five new examples of aripiprazole (arip) salts are presented, viz., the Harip phthalate [$Harip^+ \cdot C_8H_5O_4^-$ **(I)**], homophthalate [$Harip^+ \cdot C_9H_7O_4^-$ **(II)**] and thiosalicilate [$Harip^+ \cdot C_7H_4O_2S^-$ **(III)**] salts on one side, and two different dihidrogenphosphates, $Harip^+ \cdot H_2PO_4^- \cdot 2(H_3PO_4) \cdot H_2O$ **(IV)** and $Harip^+ \cdot H_2PO_4^- \cdot H_3PO_4$ **(V)**. Regarding the internal structure of the $aripH^+$ cations, they do not differ from the already known moieties in bond distances and angles, while interesting differences in conformation can be observed, setting them apart in two groups: those in **I**, **II** and **III** present similar conformations to those in the so far reported arip salts presenting the same centrosymmetric $R(8)_2^2$ dimeric synthon, but different to those in **IV** and **V**. In parallel, the anion (+ acid) groups define bulky systems of different dimensionality (1D in the former group, 2D in the latter). The correlation between arip molecular conformation and anionic network type is discussed. An interesting feature arises with the water solvato molecule in **IV**, disordered around an inversion center, in regard with its interaction with an (also disordered) phosphato O–H, in a way that an "orderly disordered" H-bonding scheme arises, complying with the S.G. symmetry requirements only on average.

Introduction

Aripiprazole (7-[4-[4-(2,3-di-chlorophenyl)-1-piperazinyl]butoxy]-3,4-dihydro-2 (1H)-quinolinone (hereafter arip) is an antipsychotic drug, perhaps the most relevant representative of a modern family of atypical antipsychotics, with a different therapeutic activity to those of the classical antipsychotic drugs of standard use (see, for instance Ref. [1]).

The drug crystallizes in a number of forms, either purely polymorphic [2–4] or as ethanol, methanol–water, dichloroethane solvatomorphs [5].

The first structural reports on arip salts were those on aripiprazolium nitrate **(1)** [6], perchlorate **(2)** [7], and oxalate **(3)** [8], further complemented by the benzoic **(4)**, 2,4-di-hydroxy-benzoic **(5)**, 2,5-di-hydroxy-benzoic **(6)** and hydrochloric **(7)** acid salts [9].

All these latter compounds present the same protonated state of the arip ligand, at the nitrogen atom attached to the alkyl chain. In addition, arip presents an H-bonding donor (the amido N–H) which in all the salts known so far serve to join neighboring arip molecules through any of two well defined supramolecular synthons, viz., some variants of a C(4) catemer, on one side, or a centrosymmetric $R(8)_2^2$ diamide ring (for Graph set nomenclature, see Ref. [10]). Nanubolu and coworkers noticed that the first of these synthons seems to group the structures containing the smaller inorganic counterions (NO_3^- **(1)**, ClO_4^- **(2)** and Cl^- **(7)**), while the second is preferred by the larger aromatic acid derivatives.

* Corresponding author. Tel.: +54 11 67727097.
E-mail addresses: freire@tandar.cnea.gov.ar (E. Freire), baggio@cnea.gov.ar (R. Baggio).
[1] Member of Consejo Nacional de Investigaciones Científicas y Técnicas, Conicet.

http://dx.doi.org/10.1016/j.molstruc.2014.03.062
0022-2860/

Table 1
Experimental details.

	(**I**)	(**II**)	(**III**)	(**IV**)	(**V**)
Chemical formula	$C_{23}H_{28}Cl_2N_3O_2{\cdot}C_8H_5O_4$	$C_{23}H_{28}Cl_2N_3O_2{\cdot}C_9H_7O_4$	$C_{23}H_{28}Cl_2N_3O_2{\cdot}C_7H_4O_2S$	$C_{23}H_{28}Cl_2N_3O_2{\cdot}2(H_3O_4P){\cdot}H_2O_4P{\cdot}H_2O$	$C_{23}H_{28}Cl_2N_3O_2{\cdot}H_2O_4P{\cdot}H_3O_4P$
M_r	614.50	628.53	601.55	760.37	644.36
Crystal system, space group	Monoclinic, $P2_1/c$	Monoclinic, $P2_1/c$	Monoclinic, $P2_1/c$	Monoclinic, $P2_1/n$	Monoclinic, $C2/c$
Temperature (K)	294	294	294	294	294
a, b, c (Å)	14.8535 (4), 9.7431 (3), 21.3861 (8)	14.7856 (7), 10.3895 (5), 21.1779 (11)	15.1735 (4), 9.6570 (3), 21.3324 (7)	17.725 (4), 8.4492 (17), 22.230 (4)	17.1053 (3), 9.18948 (14), 37.1817 (7)
β (°)	106.922 (3)	109.339 (6)	107.460 (3)	94.05 (3)	102.7748 (17)
V (Å^3)	2960.98 (17)	3069.7 (3)	2981.82 (16)	3320.8 (11)	5699.88 (16)
Z	4	4	4	4	8
Radiation type	Mo Kα	Mo Kα	Mo Kα	Mo Kα	Mo Kα
μ (mm^{-1})	0.27	0.26	0.33	0.41	0.40
Crystal size (mm)	0.32 × 0.08 × 0.02	0.24 × 0.18 × 0.12	0.28 × 0.12 × 0.10	0.30 × 0.10 × 0.06	0.22 × 0.20 × 0.15
Crystal shape	Needle	Prism	Prism	Needle	Block
T_{min}, T_{max}	0.96, 0.99	0.95, 0.97	0.94, 0.97	0.95, 0.98	0.91, 0.94
No. of measured, independent and observed [$I > 2\sigma(I)$] reflections	16895, 6871, 3520	16,630, 6898, 3683	25,900, 7133, 5309	13,815, 7506, 4734	67,354, 7191, 6284
R_{int}	0.043	0.083	0.036	0.072	0.031
$(\sin\theta/\lambda)_{max}$ (Å^{-1})	0.685	0.671	0.686	0.679	0.687
$R[F^2 > 2\sigma(F^2)]$, $wR(F^2)$, S	0.061, 0.112, 1.00	0.048, 0.073, 0.94	0.059, 0.154, 1.14	0.056, 0.148, 1.00	0.054, 0.113, 1.21
No. of reflections	6871	6898	7133	5830	7191
No. of parameters	389	398	374	459	389
No. of restraints	3	3	1	27	7
Weighting scheme	$w = 1/[\sigma^2(F_o^2) + (0.0232P)^2]$ where $P = (F_o^2 + 2F_c^2)/3$	$w = 1/[\sigma^2(F_o^2) + (0.0072P)^2]$ where $P = (F_o^2 + 2F_c^2)/3$	$w = 1/[\sigma^2(F_o^2) + (0.0515P)^2 + 2.851P]$ where $P = (F_o^2 + 2F_c^2)/3$	$w = 1/[\sigma^2(F_o^2) + (0.0798P)^2 + 0.1782P]$ where $P = (F_o^2 + 2F_c^2)/3$	$w = 1/[\sigma^2(F_o^2) + (0.0234P)^2 + 12.5359P]$ where $P = (F_o^2 + 2F_c^2)/3$
Δ>max, Δ>min (e Å^{-3})	0.32, −0.29	0.28, −0.21	0.90, −0.66	0.28, −0.29	0.65, −0.51

Data collection: Oxford Diffraction Gemini CCD S Ultra diffractometer; absorption correction: multi-scan, in CrysAlis PRO [14]. Structure resolution, SHELXS-97 [15], Structure Refinement: SHELXL-97 [15], Molecular Graphics: SHELXTL [15].

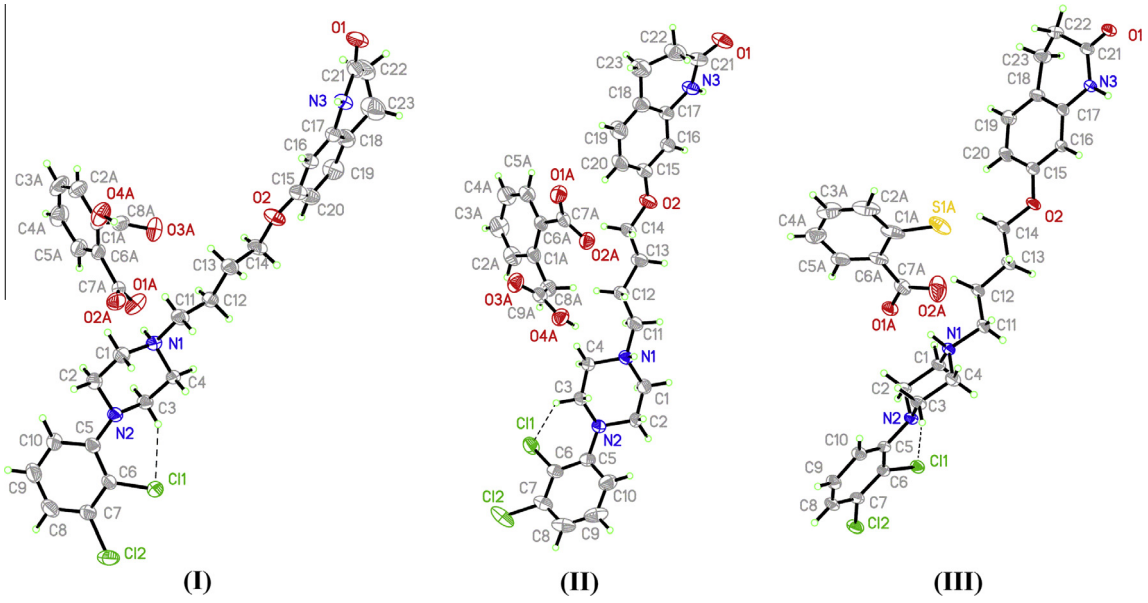

Fig. 1. Ellipsoid plot of structures **I**, **II** and **III**, drawn at a 40% probability level. In broken lines, the intramolecular C–H···Cl interaction.

We present herein five new examples of arip salts which provide a different insight into the factors deciding the packing setup and molecular conformation, viz., the Harip phthalate [Harip$^+{\cdot}C_8H_5O_4^-$ (**I**)], homophthalate [Harip$^+{\cdot}C_9H_7O_4^-$ (**II**)] and thiosalicilate [Harip$^+{\cdot}C_7H_4O_2S^-$ (**III**)] salts on one side, and two different dihidrogenphosphates, Harip$^+{\cdot}H_2PO_4^-{\cdot}2(H_3PO_4){\cdot}H_2O$ (**IV**) and Harip$^+{\cdot}H_2PO_4^-{\cdot}H_3PO_4$ (**V**). In all these complexes the leading synthon is the $R(8)_2^2$ diamide ring, and the anion (+acid) groups

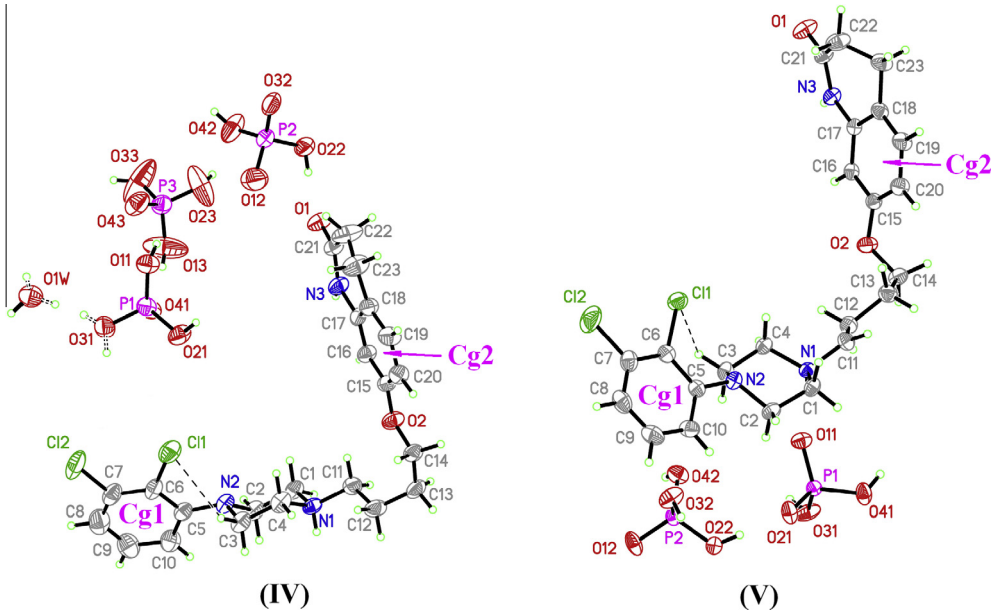

Fig. 2. Ellipsoid plot of structures **IV** and **V**, drawn at a 40% probability level. In broken lines, the intramolecular C–H···Cl interaction.

Table 2
Hydrogen-bond geometry (Å, °) for (**I**).

(**I**)	*D*–H···*A*	H···*A*	*D*···*A*	*D*–H···*A*
	C3–H3*B*···Cl1	2.63	3.215 (3)	119
	N3–H3···O1^{i}	2.07 (2)	2.922 (3)	178 (2)
	N1–H1···O2*A*	1.76 (1)	2.612 (3)	168 (2)
	O4*A*–H4*A*···O1*A*^{ii}	1.71 (2)	2.553 (3)	167 (3)
	C2*A*–H2*A*1···O1^{iii}	2.53	3.293 (3)	140
	C1–H1*A*···O3*A*^{ii}	2.53	3.328 (3)	139
	C4–H4*B*···O4*A*^{iv}	2.54	3.349 (3)	141
Symmetry codes: (i) −*x*, −*y* + 2, −*z* + 1; (ii) −*x* + 1, *y* − 1/2, −*z* + 1/2; (iii) −*x*, *y* − 1/2, −*z* + 1/2; (iv) −*x* + 1, *y* + 1/2, −*z* + 1/2.				
(**II**)	D–H···A	H···A	D···A	D–H···A
	C3–H3*B*···Cl1	2.67	3.241 (3)	118
	N1–H1···O2*A*^{i}	1.74 (2)	2.600 (3)	169 (3)
	N3–H3···O1^{ii}	2.06 (2)	2.910 (4)	179 (3)
	O4*A*–H4*A*···O1*A*^{i}	1.72 (1)	2.577 (3)	173 (3)
	C1–H1*A*···*Cg*2^{iii}	2.71	3.459 (3)	134
	C23–H23*B*···*Cg*1^{iv}	2.81	3.742 (4)	162
Symmetry codes: (i) −*x* + 1, *y*−1/2, −*z* + 1/2; (ii) −*x*, −*y* + 1, −*z* + 1; (iii) *x*, *y* − 1, *z*; (iv) *x* − 1, *y* + 1, *z*. Ring codes: Cg1, C5 → C10; Cg2, C1A → C6A				
(**III**)	D–H···A	H···A	D···A	D–H···A
	C3–H3*B*···Cl1	2.64	3.221 (2)	119
	N3–H3···O1^{i}	2.07 (3)	2.921 (3)	173 (3)
	N1–H1···O1*A*	1.89 (3)	2.770 (3)	174 (3)
	N1–H1···O2*A*	2.48 (3)	3.079 (3)	125 (2)
	C2*A*–H2*A*2···O1^{ii}	2.44	3.361 (4)	169
	C4–H4*B*···S1*A*^{iii}	2.81	3.683 (2)	150
Symmetry codes: (i) −*x*, −*y* + 2, −*z* + 1; (ii) −*x*, *y*−1/2, −*z* + 1/2; (iii) −*x* + 1, *y* + 1/2, −*z* + 1/2.				
(**IV**)	*D*–H···*A*	H···*A*	*D*···*A*	*D*–H···*A*
	C3–H3*B*···Cl1	2.76	3.269 (4)	114
	N3–H3···O1^{i}	2.18 (3)	2.995 (4)	160 (3)
	C4–H4*B*···Cl1^{ii}	2.81	3.458 (3)	125
	O11–H11···O43	1.87 (3)	2.582 (4)	141 (3)
	O21–H21···O32^{iii}	1.76 (2)	2.538 (4)	152 (4)
	O42–H42···O11^{iv}	1.74 (3)	2.583 (4)	174 (3)
	O13–H13···O41	1.68 (4)	2.509 (4)	168 (5)
	O33–H33···O23^{iv}	1.81 (4)	2.486 (7)	135 (4)
	O23–H23···O12	1.87 (2)	2.610 (4)	144 (4)
	O1*W*–H1*WA*···O32^{iv}	2.02 (3)	2.754 (4)	145 (3)
	O1*W*–H1*WB*···O31	1.90 (2)	2.732 (4)	166 (5)
	O1*W*–H1*WC*···O1*W*^{v}	1.94 (4)	2.775 (4)	170 (3)
	O31–H31*B*···O1*W*	1.90 (2)	2.732 (4)	167 (5)
	O31–H31*A*···O31^{vi}	1.88 (5)	2.715 (4)	168 (4)
	N1–H1···O41^{ii}	1.86 (2)	2.706 (3)	174 (3)
	O22–H22···O1	1.72 (2)	2.558 (3)	175 (3)

(*continued on next page*)

Table 2 (*continued*)

(**I**)	*D*–H···*A*	H···*A*	*D*···*A*	*D*–H···*A*
Symmetry codes: (i) −*x* + 1, −*y* + 1, −*z*; (ii) −*x* + 3/2, *y* + 1/2, −*z* + 1/2; (iii) −*x* + 1/2, *y* + 1/2, −*z* + 1/2; (iv) −*x* + 1/2, *y*−1/2, −*z* + 1/2; (v) −*x* + 1, −*y*, −*z* + 1; (vi) −*x* + 1, −*y* + 1, −*z* + 1				
(**V**)	*D*–H···*A*	H···*A*	*D*···*A*	*D*–H···*A*
	C3–H3*B*···Cl1	2.63	3.190 (3)	117
	N3–H3···O1^{i}	2.07 (2)	2.893 (3)	165 (3)
	C2–H2*B*···O2^{ii}	2.47	3.204 (3)	132
	C4–H4*B*···O1^{iii}	2.37	3.320 (3)	166
	C8–H8···*Cg*2^{iv}	2.90	3.797 (3)	162
	C23–H23*A*···*Cg*2^{v}	2.90	3.659 (4)	136
	O31–H31···O11^{vi}	1.76 (3)	2.604 (3)	174 (3)
	O22–H22···O21	1.67 (2)	2.521 (3)	178 (4)
	O32–H32···O21^{vii}	1.70 (3)	2.529 (3)	166 (3)
	O41–H41···O12^{viii}	1.77 (3)	2.605 (3)	170 (4)
	O42–H42···O12^{ix}	1.72 (2)	2.564 (3)	177 (2)
	N1–H1···O11	1.83 (2)	2.678 (3)	176 (3)

Symmetry codes: (i) −*x*, *y*, −*z* + 3/2; (ii) *x* + 1/2, *y*−1/2, *z*; (iii) −*x* + 1/2, *y*−1/2, −*z* + 3/2; (iv) −*x* + 1/2, −*y* + 3/2, −*z* + 1; (v) −*x* + 1, −*y* + 1, −*z* + 1; (vi) *x*, *y* + 1, *z*; (vii) −*x* + 1/2, −*y* + 1/2, −*z* + 1; (viii) *x* + 1/2, *y*−3/2, *z*; (ix) −*x* + 1/2, *y* + 1/2, −*z* + 3/2 Ring code: Cg2, C15 → C20

Table 3
π–π (Å, °) for (IV).

Group 1/Group 2	ccd (Å)	da (°)	sa (°)	cpd (Å)
Cg1···Cg2^{vii}	4.044 (2)	12.11 (16)	21.2 (18)	3.77 (5)
Cg2···Cg2^{viii}	4.109 (2)	0	22.20	3.805 (2)

ccd: Center-to-center distance; cpd: center to plane distance; da: dihedral angel; sa: slippage angle (Angle subtended by the intercentroid vector to the plane normal). Symmetry codes: (vii) 3/2 − x, −1/2 + y, 1/2 − z; (viii) 1 − x, 2 − y, −z Ring codes, Cg1: C5 → C10; Cg2: C15 → C20

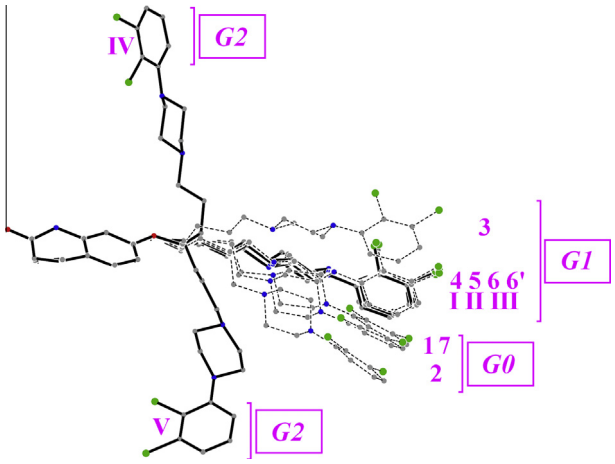

Fig. 3. Overlapping diagram of the arip molecules in all known arip salts. For structure codes and group symbols see text.

define bulky systems of different dimensionality. We shall show that the molecular conformation is closely associated to these different anionic spatial arrangements.

Experimental

Synthesis and crystallization

Aripiprazol was provided by Laboratorios Maprimed, while the remaining chemicals were of commercial origin and used as purchased.

Aripiprazol (1.5.10–4 mol, 67 mg) was dissolved in a boiling mixture of methanol (5 ml) and acetone (0.5 ml) (Compounds **I**, **II**, **IV**, **V**) or pure acetone (Compound **III**). When dissolution was considered finished, different amounts of the corresponding acids were added, as follows:

(I): 32 mg of phthalic acid was added and the resulting solution left to cool down. Crystals of **I** suitable for X-ray diffraction, in the form of colorless prisms, appeared in hours.
(II): 23 mg of thiosalicilic acid was added and the resulting solution left to cool down to 32 °C in a laboratory oven. Crystals of **II**, in the form of pale yellow prisms, showed in a few hours, but were allowed to grow for a week.
(III): 23 mg of thiosalicilic acid was added and the resulting solution left to cool down to 32 °C in a laboratory oven. Crystals of **III** in the form of pale yellow prisms were obtained in a few days.
(IV): an excess of H_3PO_4(c) was added drop wise and the resulting solution left to cool down slowly. In the term of a week excellent crystals of **IV**, were obtained as colorless prisms.
(V): to an aliquot of 1:5 aqueous dilution of H_3PO_4(c) was added and the resulting solution left to cool down slowly. Colorless prismatic crystals of **V** grew in a couple of days.

In all cases, the resulting material was used as obtained, without further recrystallization.

Refinement

Crystal data, data collection and structure refinement details are summarized in Table 1. All H atoms included in the models were found in difference maps; those attached to N/O were further refined, to end up with distance and U(iso) ranges of 0.852 (10)–0.883 (9) Å and 0.036 (8)–0.097 (4) Å^{-2}, respectively; those attached to C were instead idealized and allowed to ride, C–H (methylene), 0.97 Å; C–H (aromatic), 0.93 Å; [U_{iso}(H) = 1.2 × U_{eq} (C)]. In structure **III** the thiosalicilate counteranion appears disordered into a main, clearly defined moiety and a "ghost" image only discernable by its S atom, which was accordingly the only atom included in the model representing this minor fraction (occupations: 0.924 (2), 0.076 (2)). In order to enable convergence in the L.S refinement, similarity restraints for the S displacement factors were applied. In structure **IV** the water solvate appears disordered, with a pseudo 180° rotational disorder around the O1 W–H1 WA bond. Similarly, the H atom attached to O31 is split into two

Table 4
Selected torsion angles and complementary information on the whole set of known arip salts.

	T1 (°)	T2 (°)	T3 (°)	T4 (°)	Cl2···O1 (Å)	Cl1···O1^{i} (Å)	(i)	P.I.
1	171.9	178.2	69.0	169.4	19.28	–	–	70.6
2	167.5	178.9	70.9	172.7	18.83	–	–	69.2
3	−77.1	−171.1	−170.7	163.6	20.17	–	–	67.3
4	173.0	179.7	179.1	−164.9	20.29	2.96	1−x, −y, 1−z	66.6
5	176.9	−178.0	178.1	−160.4	20.29	2.92	2−x, 1−y, −z	64.8
6	179.1	−179.7	179.0	−160.1	16.20	2.90	x, y, 1 + z	67.9
6′	175.8	−178.9	175.6	−162.7	20.38	2.87	x, y, −1 + z	67.9
7	−178.2	−170.9	−74.8	−166.0	19.42	3.06	2−x, 1/2 + y,5/2−z	67.8
I	173.5	−180.0	175.1	−166.6	20.31	2.96	1−x, 2−y, 1−z	67.8
II	176.5	−177.5	176.1	−163.4	20.40	3.09	1−x, 1−y, 1−z	67.3
III	176.7	−179.9	178.2	−161.9	20.43	2.92	1−x, 2−y,1−z	66.6
IV	−179.1	65.1	−78.5	179.6	11.22	–	–	67.3
V	86.5	73.1	174.9	175.2	14.21	–	–	68.1

T1: C15–O2–C14–C13; T2: O2–C14–C13–C12; T3: C14–C13–C12–C11; T4: C13–C12–C11–N1 – P.I.: packing indices, as calculated by PLATON [12]°

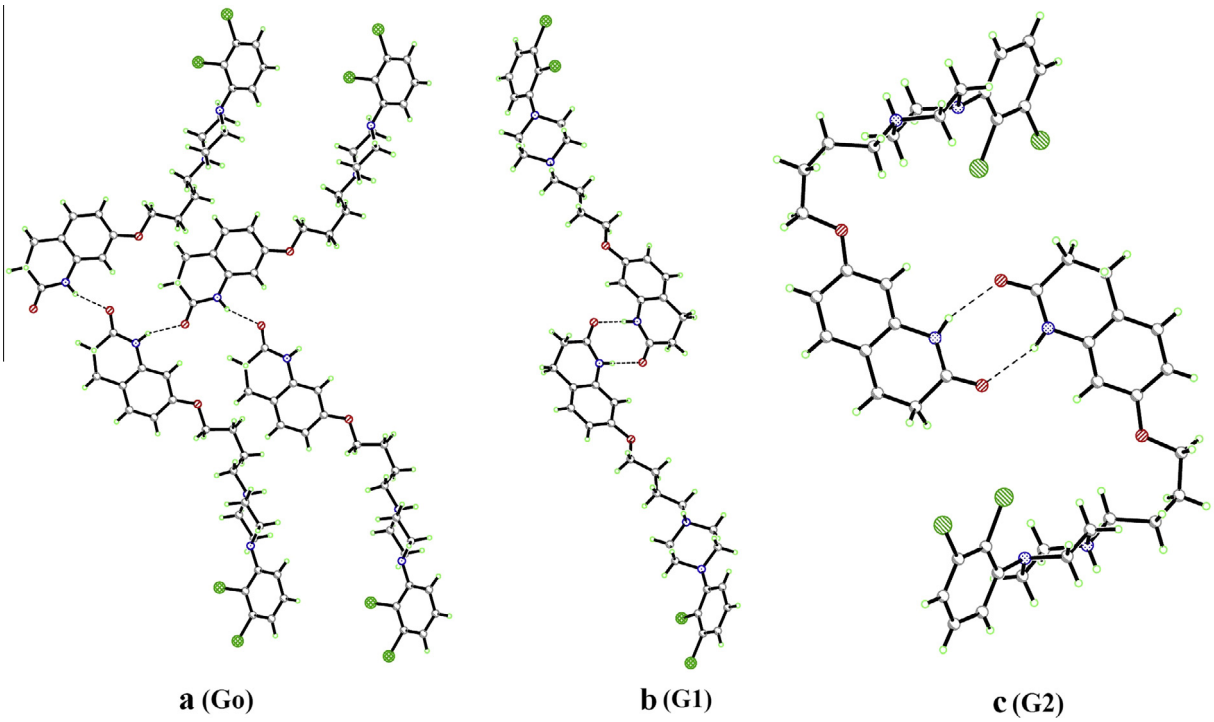

Fig. 4. Different synthons in arip salts (corresponding to the **G0**, **G1** and **G2** groups presented in Fig. 3) and the structures they give raise to.

Table 5
Comparison of cell dimension in structures 4-III.

	4	**5**	**6**[a]	**I**	**II**	**III**
A	14.9688 (10)	15.1552 (8)	30.4165 (19)	14.8535 (4)	14.7856 (7)	15.1735 (4)
B	9.9536 (6)	9.5732 (5)	9.7801 (6)	9.7431 (3)	10.3895 (5)	9.6570 (3)
C	20.9154 (14)	21.5283 (11)	20.5636 (13)	21.3861 (8)	21.1779 (11)	21.3324 (7)
B	108.0040 (10)	103.8870 (10)	105.3190 (10)	106.922 (3)	109.339 (6)	107.460 (3)
V	2963.7 (3)	3032.1 (3)	5899.8 (6)	2960.98 (17)	3069.7 (3)	2981.82 (16)
S.G.	P21/c	P21/c	P21/c	P21/c	P21/c	P21/c
Z	4	4	8	4	4	4

[a] Double cell with two independent moieties.

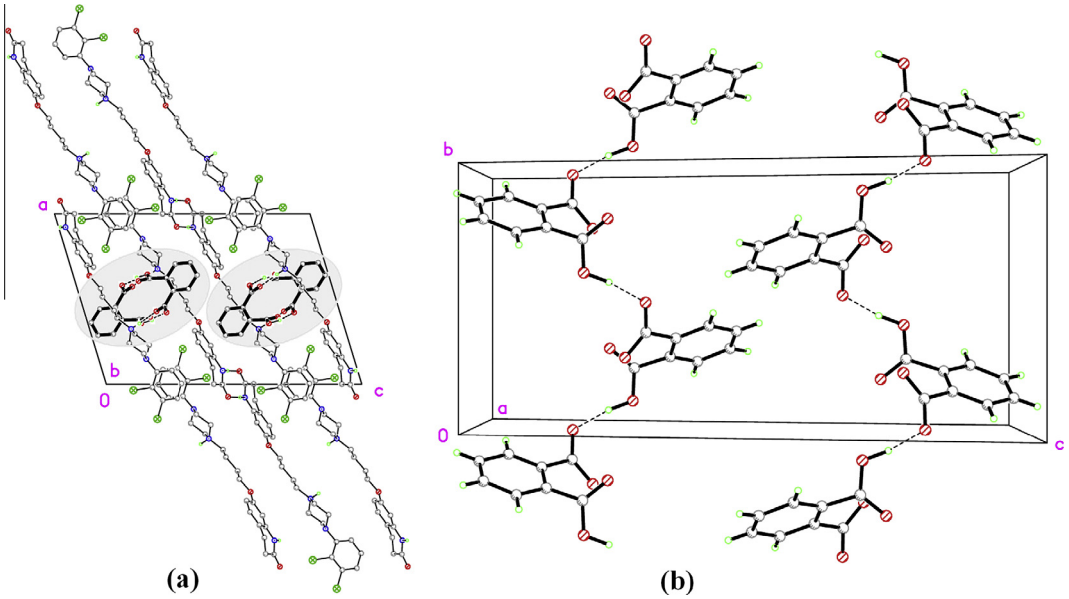

Fig. 5. Packing details for structure **I** (but extensible to **II** and **III**). (a) Viewed down b. Highlighted, in projection, the columnar anionic arrays around which the helical arrays build up. (b) A detailed view of the anionic chains.

moieties. These two kinds of disorder are linked by the H-bonding Scheme (see main text for details).

Results and discussion

Figs. 1 and 2 show ellipsoid plots of structures **I**–**III** and **IV**–**V**, respectively; Table 1 presents crystallographic and refinement data, Table 2, H-bonding interactions and Table 3, relevant π···π contacts.

In all cases the asymmetric unit consist of an Harip$^+$ cation balanced by the corresponding (1-) counteranion (phthalate **(I)**, homophthalate **(II)**, thiosalicilate **(III)**; dihydrogenphosphate **(IV, V)**. In the latter two cases this is completed by two neutral phosphoric acid molecules and one water molecule (**IV**) or by just one single phosphoric acid molecule **(V)**.

Regarding the internal structure of the Harip$^+$ cations, they do not differ from the already known moieties in what interatomic bond distances and angles concerns: they are extremely similar, including an intramolecular C–H···Cl interaction (Table 2, first entries for all structures) characteristic for the indichlorophenyl-1-piperazinyl group in all reported arip variants known to date. Due to lack of any real novelty these internal details will not be discussed any further.

More interesting are the molecular conformations; Fig. 3 presents a comparative overlap of all the known structures, which for future reference we shall collect according to their similarities in three different groups: the already reported **1**, **2** and **7** (group G0), the also known structures **3**–**6** as well as the herein presented **I**–**III** (group G1) and finally, **IV** and **V** (group G2).

It is apparent that those in group G2 differ drastically from the remaining three structures herein reported (**I**, **II**, **III**) as well as from all the remaining ones: the molecule adopts in **IV** and **V** a more bent, and accordingly closer, disposition; this is easily confirmed, for instance, by the much shorter intramolecular distance separating the outermost atoms Cl2 and O1, viz: 11.22 (2) in **IV** and 14.21 (2) Å in **V**, as compared to the rest, spanning the range 18.83 (2)–20.43 (2) Å (save one of the two independent moieties in structure **6**, an outlier of 16.20 (2) Å) (Table 4, 6th column). The "rupture zone" locates in the vicinity of the N1, C11, C12, C13, C14, O2, C15 chain, as confirmed by the dissimilar torsion angles in this region (Table 4, columns 2 to 5).

The amido N–H···O H-bonds generate in all five structures diamido $R(8)_2^2$ closed dimers (Fig. 4b and c). Similar interconnections have already been found in the remaining arip salts in group

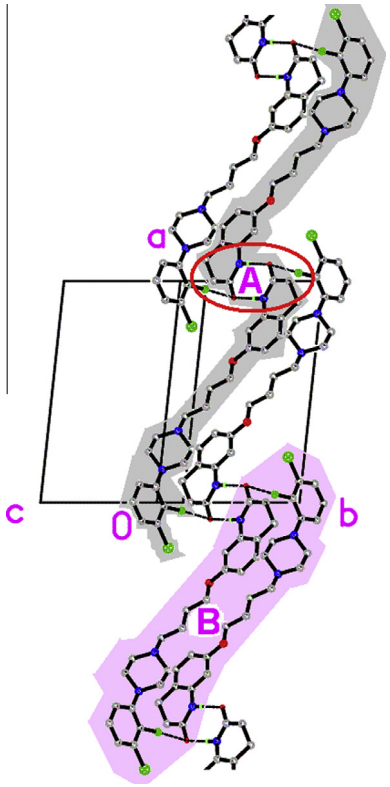

Fig. 6. The two dimeric structures in **I**. Highlighted in grey, the $R(8)_2^2$ dimer; in pink, the one promoted by the Cl···O interactioin. Labels **A** and **B** locate the inversion centers around which both dimers evolve. (For interpretation of the references to colour in this figure legend, the reader is referred to the web version of this article.)

G1: 3, **4**, **5**, **6** (those with larger counterions) and in contraposition to the C(4) catemeric synthon found in those in **G0: 1**, **2**, **7** (Fig. 4a).

Structures **I**, **II**, **III**

They configure with structures **4**, **5** and **6** a quasi- isostructural group, with rather similar cell dimensions and the same space groups (see Table 5). In fact, the apparent departure of structure **6** from this rule consists just in the inclusion of two independent moieties in the asymmetric unit with the corresponding doubling of one cell parameter. The general properties of these structures have already been treated in detail in [9] and accordingly we concern ourselves with the crystal packing. As a common feature, they all have a similar charge assisted N(+)–H···O H-bond between cation and anion, and a strong O–H···O, a weak C–H···O, or both, interactions complementing the former. These contacts give raise to isostructural helices with an Harip^{+} plus acid^{-} motif, propagating along b and riding onto the monoclinic screw axis. These helices have a central 1D column (Fig. 5a, highlighted) made up of H-bonded acid (or acid + water) chains, around which the helix evolves (Fig. 5b).

An interesting feature in **I**, **II**, **III**, seemingly overlooked in Nabubolu's work for structures **4**, **5**, **6**, is the presence of a short Cl1···O1 contact (Table 4 , 7th and 8th columns), much shorter than the sum of the corresponding sum of van der Waal's radii (3.27 Å), according to Bondi [11]. This interactions and the N–H···O H-bonds generating the $R(8)_2^2$ dimeric structures (Fig. 6, grey highlight) have the same O1 atom in common, as well as the inversion center around which they evolve (Fig. 6, "A"). These Cl···O interactions generate new dimeric substructures (Fig. 6, pink highlight) centered around a second inversion center (Fig. 6, "B") and provide for an extra lateral link between [0 1 0] helices.

Structures **IV** and **V**

As ditto, structures in group G2 are radically different to all previously reported arip salts (Groups G0 and G1); even if also here the $R(8)_2^2$ dimers are the structural cationic leitmotifs as in **I**–**II**–**III**, they have a different shape and interact in a different way. Another distinctive feature is the tight anionic networks building up out of H-bonding. Due to these singularities these structures will be treated in detail.

In the case of **IV** the anionic substructure is shown in Fig. 7a; it consists of a broad planar array parallel to $(\bar{1}\,0\,1)$ passing through the cell origins. It is formed by a very dense H-bonding network sustained by O–H···O bonds involving dihidrogenphosphates anions, phosphoric acid molecules and water solvates.

Entries 4 → 10 in Table 2-**IV** correspond to ordered, well defined H-bonding interactions, needing no special description besides the tabular information. There is, however, a special zone, parallel to the ***b*** axis and represented in grey in Fig. 7a, where H atoms appear

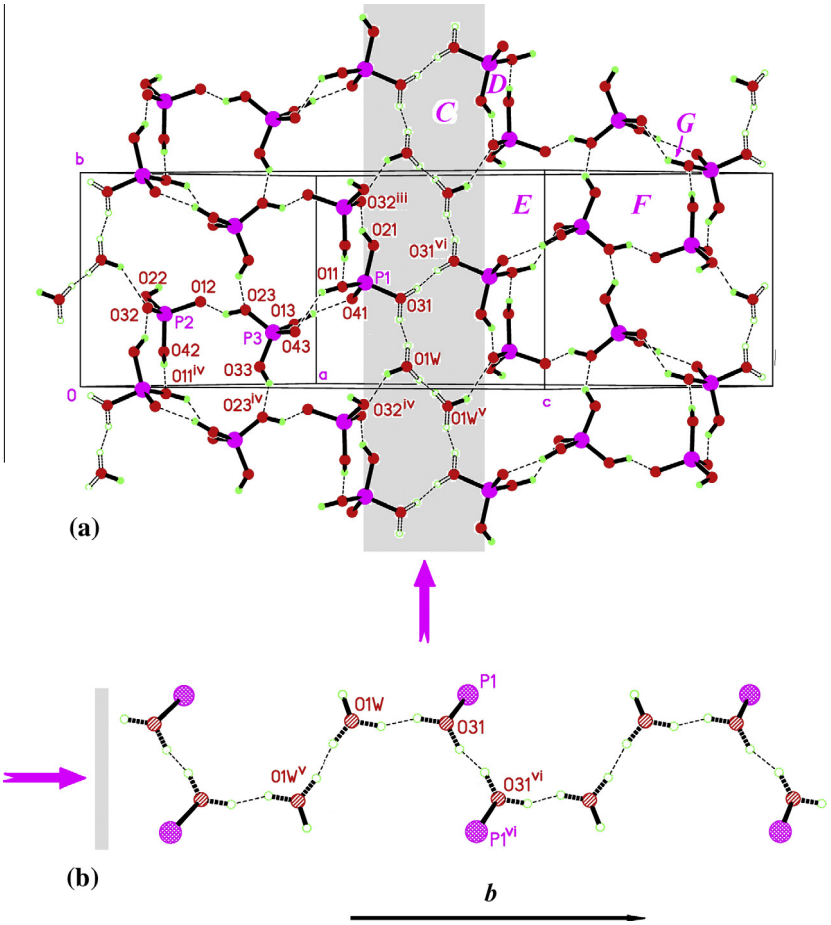

Fig. 7. Packing diagram of **IV** showing: (a) the $(\bar{1}\,0\,1)$ anionic layers made up of $H_2PO_4^-$ anions and (H_3PO_4) and H_2O molecules. Highlighted, the "orderly-disordered" H-bonding chain involving the water solvate and one of the phosphoric acid molecules. (b) A detailed vew of the former chain. Symmetry codes: (i) $-x+1, -y+1, -z$; (ii) $-x+3/2, y+1/2, -z+1/2$; (iii) $-x+1/2, y+1/2, -z+1/2$; (iv) $-x+1/2, y-1/2, -z+1/2$; (v) $-x+1, -y, -z+1$; (vi) $-x+1, -y+1, -z+1$.

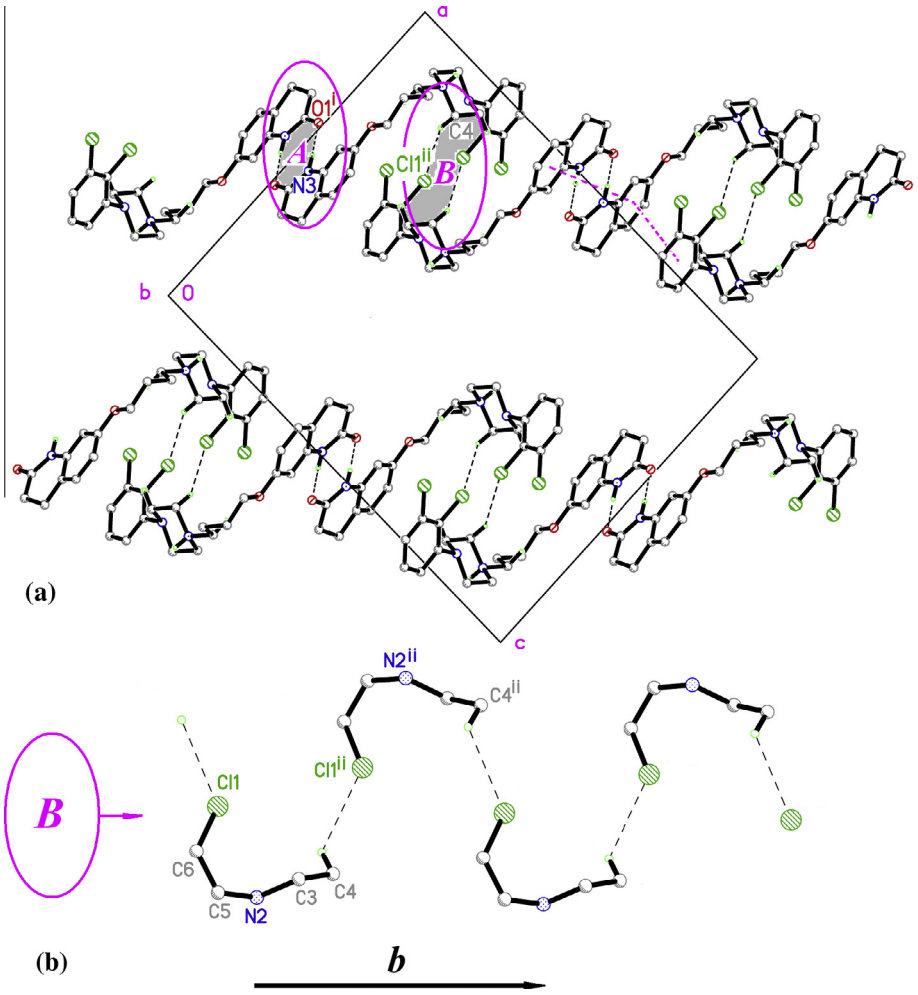

Fig. 8. Packing diagram of **IV** showing the $(\bar{1}\,0\,1)$ cationic layers, made up of Harip + ions. (a) In a [0 1 0] projection showing the linkage between Harip molecules. The shaded region A corresponds to the $R(8)_2^2$ loop while B corresponds to the C(7) H-bonded chain. (b) A schematic explanation of the way in which the latter chain operates along b. Symmetry codes: (i) $-x+1, -y+1, -z$; (ii) $-x+3/2, y+1/2, -z+1/2$.

disordered (split in equally populated halves), and alternate so as to complete a well connected chain, but abiding to S.G. symmetry only on average. The H atoms involved are H1Wb, H1Wc in O1W, and H31a, H31b in O31–P1, and the way in which the chain in built up is clarified in Fig. 7b: disordered H atoms appear in broken bonds, and occupancies are such as to avoid the short H···H contacts: when one of these H's is present, the corresponding one at "bumping distance" in the acceptor's side is absent, and the one pointing in the opposite direction is present instead. In this way a chain which preserves an "average symmetry" is possible. The disordered H-bonds involved are presented in entries 11 → 14 in Table 2-**IV**, and in spite that four entries are therein shown, they stand only for two different (disordered) interactions. This anionic array is fully supported by O–H···O bonds only, and gives raise to five different types of rings (Fig. 7a), two of them of a $R(8)_2^2$ type (Fig. 7a, D and G); one $R(12)_5^5$ (Fig. 7a, C); one $R(14)_4^3$ (Fig. 7a, F) and one $R(16)_5^5$ (Fig. 7a, E).

Regarding arip molecules, the $R(8)_2^2$ dimers (Fig. 8a, encircled zone "A") are interconnected by weak C–H···Cl interactions (3rd entry in Table 2-**IV**, and Fig. 8a, encircled zone "B"). Fig. 8b presents an extremely simplified perpendicular view showing the real character of the interaction, a C(7) helicoidal catemer linking dimers along ***b*** to form a 2D cationic structure extending parallel to $(\bar{1}\,0\,1)$, midway cell origins. The whole assembly is reinforced by the π···π contacts presented in Table 3 and shown in (magenta) broad broken lines in Fig. 8a (upper right). These cationic arrays fill the gap between anionic ones; both types of sheets stack in alternating fashion along $[\bar{1}\,0\,1]$ and only a few well defined H-bonds contribute to the interplanar linkage, mainly a strong $N–H_{(Harip)}\cdots O_{(Phosp)}$ complemented by $O–H_{(Phosp)}\cdots O_{(Harip)}$ (entries 15 → 16 in Table 2-**IV**).

Structure **V:** Somehow mimicking what observed in **IV**, the structure consists of interleaved anionic and cationic 2D networks, now parallel to (0 0 1). The former ones are made up by dihidrogenphosphato anions and phosphoric acid molecules, interlinked by the H-bonds presented as entries 5 → 9 in Table 2-**V** and shown in Fig. 9. As in **IV**, a number of H-bonding rings appear, viz., two $R(8)_2^2$ (Fig. 9, B and D); one $R(12)_4^2$ (Fig. 9, E); one $R(14)_4^3$ (Fig. 9a, C) and one $R(16)_4^4$ (Fig. 9, F).

On the other hand the cationic 2D substructure in **V** (Fig. 10) is constructed by the diamido $R(8)_2^2$ closed dimers (entry 2 in Table 2-**V** and encircled zone "A" in Fig. 10) interlinked through a complex network of weak C–H···O and C–H···π interactions (entries 3, 4 and 10,11 in Table 2-**V**). The result is a broad planar array parallel to (0 0 1), with a width ~3/8 of the whole ***c*** axis, and centered at $z \sim 0.25, 0.75$.

Cationic and anionic sheets stack also in alternating fashion, now along the [0 0 1] direction, and some well defined H-bonds

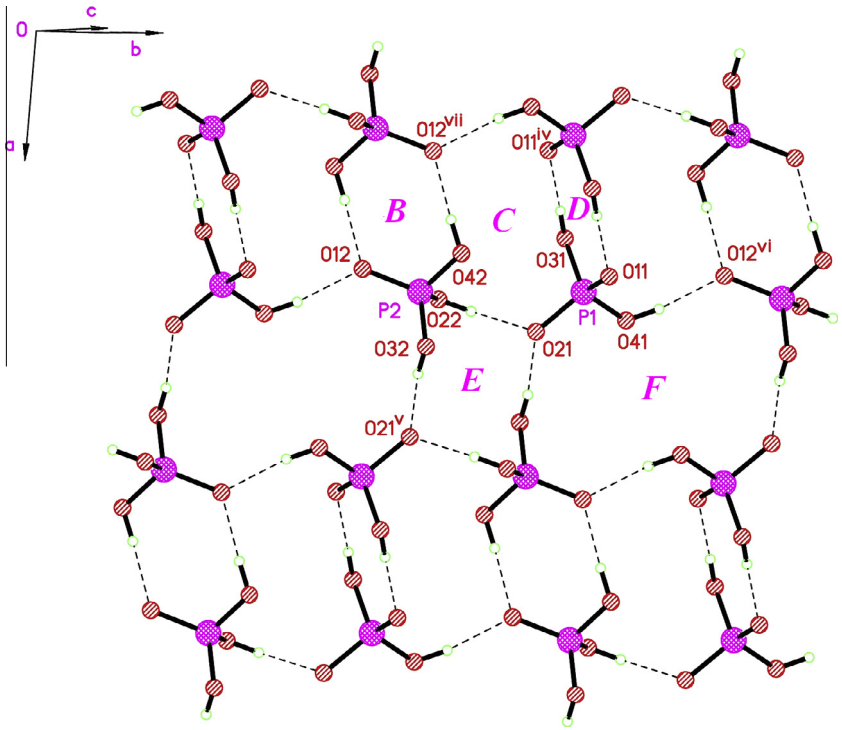

Fig. 9. Packing diagram of (001) anionic layers in V, drawn for the sake of clarity in a slightly slanted fashion. Symmetry codes: (iv) $-x+1/2, -y+3/2, -z+1$; (*v*) $-x+1, -y+1, -z+1$; (vi) $x, y+1, z$.

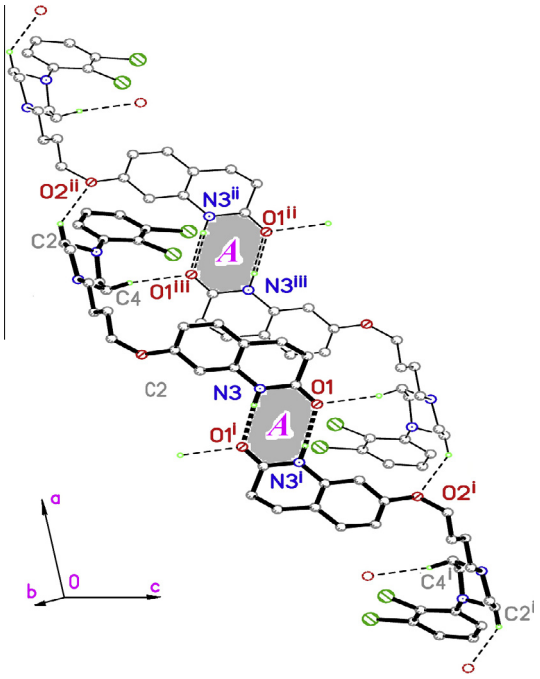

Fig. 10. Cationic 2D substructure in **V** constructed by the di-amido $R(8)_2^2$ closed dimers interlinked through a complex network of weak C–H···O and C–H···□ interactions. Symmetry codes: (i) $-x, y, -z+3/2$; (ii) $x+1/2, y-1/2, z$; (iii) $-x+1/2, y-1/2, -z+3/2$.

contribute to the linkage between sheets, mainly through a strong $N–H_{(Harip)}\cdots O_{(Phosp)}$ bond (seen in both structures, entries 15–16 in Table 2-**IV** and 12 in Table 2-**V**)

The basically similar packing arrays are presented in Figs. 11a and b: the phosphoric anionic networks are shown in bold, while the $Harip^+$ cations are shown in simple lining. The most notorious difference resides in the interlayer spacings ($d_{(2\bar{0}2)} \sim 7.163$ Å in **IV**; $d_{(002)} \sim 11.087$ Å in **V**).

Conclusion

The results already discussed allow to disclose some interesting regularities.

Fist of all, the molecular conformation of the (now expanded) family of arip salts can be classified in three clearly differentiated groups, as a natural extension of the two categories formerly suggested by Nanubolu and coworkers. The already described Fig. 3 presents them, grouped as **G0** (those derived from the smaller, inorganic acids HNO_3 **(1)**, $HClO_4$ **(2)**, HCl **(7)**); **G1**, including the quasi isostructural family of benzoic acids and derivatives (Structures **4**–**6** and **I-III**), plus oxalic acid (Structure **7**) and **G2**, those derived from phosphoric acid (**IV**, **V**).

It has already been stated that group **G0** is characterized by small acid groups filling empty spaces between arip C(4) catemers (Fig. 8a) in isolated, almost non interacting disposition, which seems to be the most appropriate for a closer packing: Table 4 presents in its last column the packing indices (P.I.) for all 12 structures, as calculated by PLATON [12] following the 1973 work by Kitajgorodskij [13], It can be seen that the **G0** group spans a P.I. range of 69.2–70.6, against 64.8–67.9 for **G1** and 67.3–68.1 for **G2**. The straightforward inference is that the C(4) syntons promoted by the small, sparcely spaced inorganic acid groups (Fig. 4a), formally describable as 0D arrays, favor more densely packed structures than the $R(8)_2^2$ dimers (Fig. 4b and c) generated by the bulkier acid structures found in the rest.

Regarding these latter ones, it is quite interesting to note that group **G1** is characterized by anionic columns (1D structures) among which arip dimeric units interleave in a rather unconstrained way, in

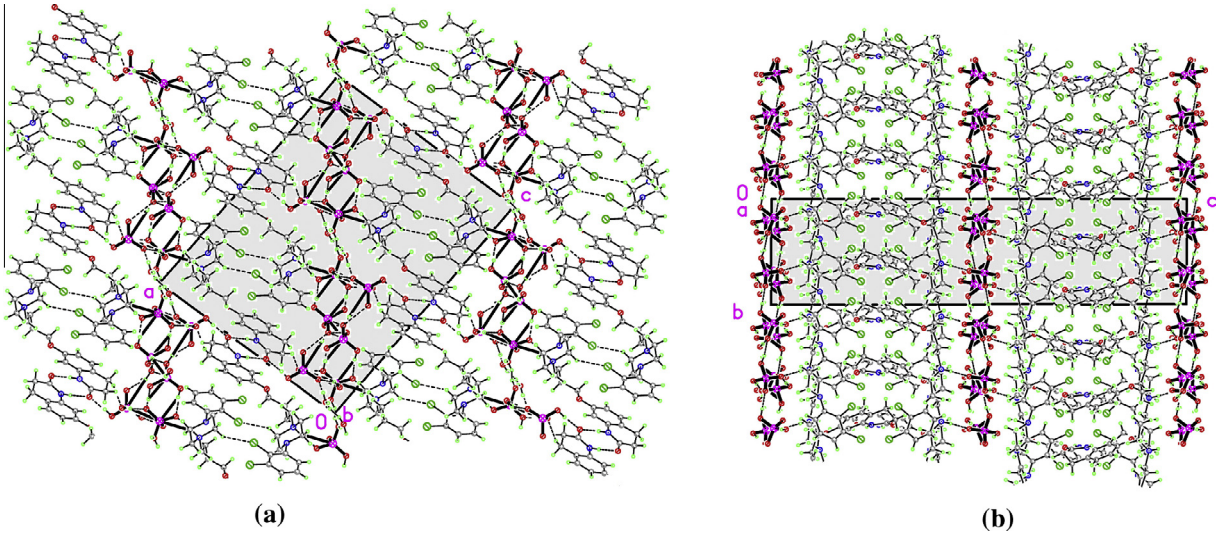

Fig. 11. Alternating stacking of cationic and anionic sheets in **IV** and **V**, viewed in projection.

order to generate the final crystal structure while group **G2** is characterized by 2D anionic/solvato networks, heavily intralinked by the strongest H-bonds present in each structure. These broad planes dispose parallel to each other in such a way as to leave in between a tightly bound 2D space finally filled by the arip dimeric substructures: the limited lateral space available may thus be the reason for the "crooked" shape of the dimers (Fig. 4c), so similar in both **G2** structures and so different to **G1** ones (Fig. 4b).

This hypothesis would give the (dimensionality of the) anionic H-bonding network a crucial role in the final shape adopted by the arip molecule in its salts, acting somehow as a "template" to which the molecule would have to adapt in order to crystallize successfully.

Acknowledgements

The authors would like to acknowledge Laboratorios Maprimed, for provision of aripiprazole, and ANPCyT (project No. PME 2006-01113) for the purchase of the Oxford Gemini CCD diffractometer.

References

[1] S.G. Potkin, A.R. Saha, M.J. Kujawa, W.H. Carson, M. Ali, E. Stock, J. Stringfellow, G. Ingenito, S.R. Marder, Arch. Gen. Psychiatry 60 (7) (2003) 681–690.
[2] L. Tessler, I. Goldberg, J. Inclusion Phenom. Macrocycl. Chem. 55 (2006) 255–261.
[3] D.E. Braun, T. Gelbrich, V. Kahlenberg, R. Tessadri, J. Wieser, U. Griesser, J. Pharm. Sci. 98 (2009) 2010–2026.
[4] J.B. Nanubolu, B. Sridhar, V.S. Phani Babu, B. Jagadeeshb, K. Ravikumar, CrystEngComm 14 (2012) 4677–4685.
[5] D.E. Braun, T. Gelbrich, V. Kahlenberg, R. Tessadri, J. Wieser, U. Griesser, Cryst. Growth Des. 9 (2009) 1054–1065.
[6] E. Freire, G. Polla, R. Baggio, Acta Cryst. C68 (2012) O170–o173.
[7] E. Freire, G. Polla, R. Baggio, Acta Cryst. C68 (2012) O235–o239.
[8] E. Freire, G. Polla, R. Baggio, Acta Cryst. C69 (2013) O186–o190.
[9] J.B. Nanubolu, B. Sridhar, K. Ravikumara, S. Cherukuvadab, Cryst. Eng. Comm. 15 (2013) 4321–4334.
[10] J. Bernstein, R.E. Davis, L. Shimoni, N.-L. Chang, Angew. Chem. Int. Ed. Engl. 34 (1995) 1555–1573.
[11] A. Bondi, J. Phys. Chem. 68 (1964) 441–451.
[12] A.L. Spek, Acta Cryst. D65 (2009) 148–155.
[13] A.I. Kitajgorodskij, Molecular Crystals and Molecules, Academic Press, New York, 1973.
[14] Oxford Diffraction. CrysAlis PRO, version 171.33.48. Oxford Diffraction Ltd., Abingdon, Oxfordshire, England, 2009.
[15] G.M. Sheldrick, Acta Cryst. A64 (2008) 112–122.